the plant journal

SEB Society for Experimental Biology

The Plant Journal (2011) **68**, 377–385 doi: 10.1111/j.1365-313X.2011.04692.x

TECHNICAL ADVANCE

High-resolution live imaging of plant growth in near physiological bright conditions using light sheet fluorescence microscopy

Alexis Maizel[1,*,†], Daniel von Wangenheim[2,†], Fernán Federici[3], Jim Haseloff[3] and Ernst H.K. Stelzer[2,*]

[1]*Department of Stem Cell Biology, Center for Organismal Studies, University of Heidelberg, Im Neuenheimer Feld 230, D-69120 Heidelberg, Germany,*

[2]*Physical Biology (FB15 IZN, CEF-MC, FMLS), Goethe Universität Frankfurt am Main, Max-von-Laue-Straße 9, D-60438 Frankfurt am Main, Germany, and*

[3]*Department of Plant Sciences, University of Cambridge, Downing Street, Cambridge CB2 3EA, UK*

Received 25 May 2011; revised 21 June 2011; accepted 24 June 2011; published online 5 August 2011.

[*]For correspondence (fax +49 6221 54 64 24; e-mail alexis.maizel@cos.uni-heidelberg.de or fax +49 69 798 29607; e-mail ernst.stelzer@physikalischebiologie.de).

[†]These authors contributed equally to this work.

SUMMARY

Most plant growth occurs post-embryonically and is characterized by the constant and iterative formation of new organs. Non-invasive time-resolved imaging of intact, fully functional organisms allows studies of the dynamics involved in shaping complex organisms. Conventional and confocal fluorescence microscopy suffer from limitations when whole living organisms are imaged at single-cell resolution. We applied light sheet-based fluorescence microscopy to overcome these limitations and study the dynamics of plant growth. We designed a special imaging chamber in which the plant is maintained vertically under controlled illumination with its leaves in the air and its root in the medium. We show that minimally invasive, multi-color, three-dimensional imaging of live *Arabidopsis thaliana* samples can be achieved at organ, cellular and subcellular scales over periods of time ranging from seconds to days with minimal damage to the sample. We illustrate the capabilities of the method by recording the growth of primary root tips and lateral root primordia over several hours. This allowed us to quantify the contribution of cell elongation to the early morphogenesis of lateral root primordia and uncover the diurnal growth rhythm of lateral roots. We demonstrate the applicability of our approach at varying spatial and temporal scales by following the division of plant cells as well as the movement of single endosomes in live growing root samples. This multi-dimensional approach will have an important impact on plant developmental and cell biology and paves the way to a truly quantitative description of growth processes at several scales.

Keywords: microscopy, light sheet, root, growth, Arabidopsis.

INTRODUCTION

Live imaging of an organism is the tool of choice for understanding the dynamics of the biological processes at work in living cells and organisms. The primary goal is to work under conditions that are close to those in nature. This requires a minimally invasive imaging method with sufficient spatial resolution and temporal capability to capture the biological events as they occur. One of the main issues is to find a trade-off between preserving the biological integrity of the specimen and acquiring images at a sufficiently high signal-to-noise ratio. For multicellular organisms, observing a whole specimen requires non-destructive sectioning in which the covered volume can be several hundred micrometers thick. Optical sectioning must keep the specimen intact and alive for well-defined periods of time and can be achieved in three fundamentally different ways: (i) by post-processing images obtained by deconvolution of wide-field microscopy (McNally *et al.*, 1999); (ii) by restricting the excitation to the plane of interest and detecting the fluorescence signal with a camera; or (iii) by illuminating the sample and physically blocking out-of-focus light by a

pinhole in front of a detector as employed in confocal microscopy and its variant spinning disk microscopy. Still, whenever a single plane is observed in a confocal or a wide-field fluorescence microscope, the entire specimen is illuminated (Verveer *et al.*, 2007). Recording stacks of images along the optical *z*-axis thus illuminates the entire specimen once for each plane, hence the sample is exposed to more light than is required for image acquisition.

Light sheet fluorescence microscopy (LSFM) uses a low-numerical-aperture lens to focus a sheet of light and to illuminate the specimen from one side while collecting the emitted light at a perpendicular axis (Figure 1A,B). The center of the illuminating light sheet and the focal plane of the detection system overlap. The thickness of the light sheet is similar to and in many instances even thinner than the depth of field of the detection system. Thus, only fluorophores close to the focal plane of the detection system are excited and contribute to the image. Intrinsically, only a fraction of the fluorophores suffer from photobleaching. The LSFM functions as a non-destructive microtome and microscope and has become increasingly popular in developmental studies. A LSFM was used to record the early development of zebrafish and flies with subcellular resolution and short sampling periods (60–90 sec per stack) (Keller *et al.*, 2008, 2010). The LSFM exposes an embryo to 200 times less energy than a conventional microscope and 5000 times less energy than a confocal fluorescence microscope (Keller *et al.*, 2008, 2010). In combination with incoherent structured illumination the contribution of scattered light to the image is reduced (Keller *et al.*, 2010). In addition, LSFM can be operated with laser cutters (Engelbrecht *et al.*, 2007) and, in conjunction with high-speed cameras that produce about 500 images per second, it can be used for fluorescence correlation spectroscopy (Wohland *et al.*, 2010).

Plants have a diverse and flexible architecture based upon relatively simple repetitive units. However, in contrast to animals, most organogenesis occurs post-embryonically and in two confined areas called meristems, which are located in the apical (shoot) and basal (root) ends of the plant. This peculiar mode of development has led to interest in studying the dynamics of organ formation and growth in a living organism. Several seminal studies have used live imaging to study the dynamics of *Arabidopsis thaliana* development. The dynamic processes relate to the specification and growth of lateral organs and to (sub)cellular processes (Boisnard-Lorig *et al.*, 2001; Reddy *et al.*, 2004; Fang and Spector, 2005; Heisler *et al.*, 2005, 2010; Paredez *et al.*, 2006; Hamant *et al.*, 2008; Laskowski *et al.*, 2008; Rybel

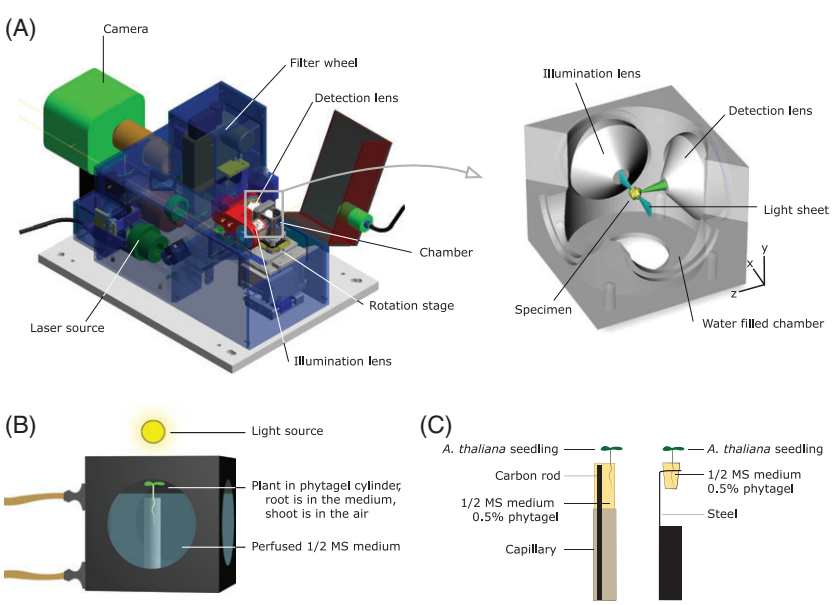

Figure 1. Light-sheet-based imaging of *Arabidopsis thaliana* seedlings.
(A) View of the central components of a digital scanned laser light sheet fluorescence microscope. The illumination system excites the fluorophores in a thin planar volume by rapidly scanning a micrometer-wide Gaussian laser beam inside the specimen. Fluorescence is collected at right angles to the illuminated plane by the detection system. The planar excitation volume and the focal plane of the detection system overlap. The intensity of the laser beam can be modulated in synchrony with the scanning process (structured illumination). Left figure by P. Theer.
(B) Close-up of the sample chamber (boxed region in A). The root of the plant is growing on the surface of a Phytagel cylinder immersed in culture medium (half-strength MS) while its leaves are in the air. The chamber is equipped with a perfusion system exchanging the whole chamber volume every 15 min and a sun-like lighting system covering the plant leaves from above.
(C) Side view of the two types of sample holder used for imaging. Left, the root of the plant grows into a 0.5% Phytagel cylinder. For the image acquisition process, the Phytagel cylinder is extruded from the capillary, which is rigidified by an embedded carbon rod. Right, the root grows through a plastic cone filled with 0.5% Phytagel maintained by a ring holder. In both designs, 2-day-old seedlings were transferred to the holders and further cultured in a tilted position such that the root grew towards the glass until the onset of imaging into the chambers indicated below.

et al., 2010). All these approaches rely on the use of deconvolution or confocal fluorescence microscopy (Fang and Spector, 2005) and immobilize the plant between a cover slip and a slide or a block of agar (e.g. Laskowski *et al.*, 2008; Rybel *et al.*, 2010) or embed the sample in agar (e.g. Reddy *et al.*, 2004; Heisler *et al.*, 2005, 2010; Hamant *et al.*, 2008) to image the sample on the horizontal stage of the microscope. This positioning is particularly problematic for an organ such as the root, the growth of which is influenced by gravity (Swarup *et al.*, 2005). In addition, since plants scatter and absorb light remarkably well, they are exposed to intense light to ensure proper illumination and detection of signals from the entire volume. The use of very high light intensities results in heating and photo-toxicity problems, which induce the malfunction and death of a specimen. Therefore, if the experimental measurements obtained are to represent normal development, there is a need to keep the sample under physiologically sustainable conditions while maintaining a high image acquisition rate.

We used light-sheet-based fluorescence microscopy in close to natural growth conditions to image live plants at the organ, cellular and subcellular scales. We show that multi-color, three-dimensional imaging of live *A. thaliana* samples can be achieved over the course of several hours. We follow and extract the growth parameters of primary root and lateral root primordia and demonstrate the applicability of our approach at varying spatial and temporal scales by recording cell division and the movement of single endosomes in live growing root samples.

RESULTS

Imaging setup

All experiments use digital scanned laser light sheet fluorescence microscopy (DSLM) (Keller *et al.*, 2008) to image a 100–300 μm thick volume of a plant by vertically scanning a thin (2–5 μm) laser beam that enters the specimen from the side (Figure 1A). The fluorescence emitted in this volume is detected with a second lens arranged at right angles to the illumination axis and imaged by a CCD camera. Three-dimensional recording is performed by moving the specimen through the illuminated plane. Multi-color acquisition is achieved with laser lines produced by diode- and diode-pumped solid state lasers and carefully selected filters to excite and observe different fluorophores serially. In DSLM the plant is placed vertically in a medium-filled chamber close to the common focal point of the two objective lenses. The leaves are maintained in the air whereas the root grows in the liquid on the surface of a gel cylinder. A perfusion system ensures that the whole chamber volume is exchanged every 15 min, therefore reducing the build-up of contaminants and toxic compounds (Figure 1B). An optional cold light source is mounted on top of the chamber. The light is provided by a lamp bank system conducting standard light intensity and color (120–150 μmol $m^{-2}sec^{-1}$, cool white) for Arabidopsis growth. During the recording process the light is turned off. Plants are germinated on half-strength MS medium and the seedlings are transferred 2 days after germination to custom-designed holders (Figure 1C) and nurtured in custom-built growth chambers (see Figure S1 in the Supporting Information). Two kinds of holders were used. In the first design, the root grows on the surface of a gel cylinder cast in a glass capillary and made rigid by a carbon rod. For imaging, a 2–5 mm long slab of the gel cylinder is extruded from the capillary, which is positioned in the microscope chamber. In a second version, a gel cone, cast in a micropipette tip, is maintained by a steel ring connected to a holder. In this design, the root grows through the gel. With this holder, the root tip can be imaged outside any gel, but maintains its natural mobility, which can be problematic for long-term recording. The mobility of the root is reduced in the first holder design (the root grows in or on the surface of the gel), but light scattering due to the gel and its influence on the quality of the image must be taken into account. To keep the influence of the gel on the imaging as low as possible we use Phytagel, also known as Gelrite. It has a higher stiffness while being clearer than other gelling agents at the same concentration (see Figure S2).

Imaging whole organs

With this setup, we recorded a growing lateral root tip of a 7-day-old transgenic Arabidopsis line stably expressing a GFP-tagged plasma membrane (LTi6–GFP) and a red fluorescent protein (RFP)-tagged nuclear marker (H2B–RFP) (Figure 2A and Movie S1). For each channel, a *z*-stack of 233 frames encompassing the entire volume of the root (300 μm) was recorded every 15 min for a total period of 38 h (Figure 2A and Movie S1). The spatial resolution achieved along the *z*-axis (i.e. the depth of the specimen) was assessed by reconstructing *xz* optical sections from the *z*-stacks (Figure 2B). Cell contours were very well resolved across the entire width of the root, in particular in the root meristem. In a cross-section of the root, the thinnest diameter of a cell wall measured was 0.77 μm (full width at half maximum). In more mature regions of the root, all concentric cell layers could be identified (pericycle, endodermis, cortex and epidermis), but cell contours in the central cylinder were less well resolved. The growth of the lateral root was variable during the recording. The growth rate was 1–2 μm h^{-1} for the first 15 h; it increased during the following 12 h to peak at 30 μm h^{-1} before dropping back to 1–2 μm h^{-1} (Figure 2C). This surge in the growth rate corresponds to the period during which the plant was illuminated, with the maximum growth rate detected 1–2 h after dusk, after which growth is inhibited. We also noted that the intensity of the LTi6–GFP membrane signal and the plant growth rate were correlated. During the initial growth lag phase, the LTi6–GFP signal dropped to later increase concomitantly with the

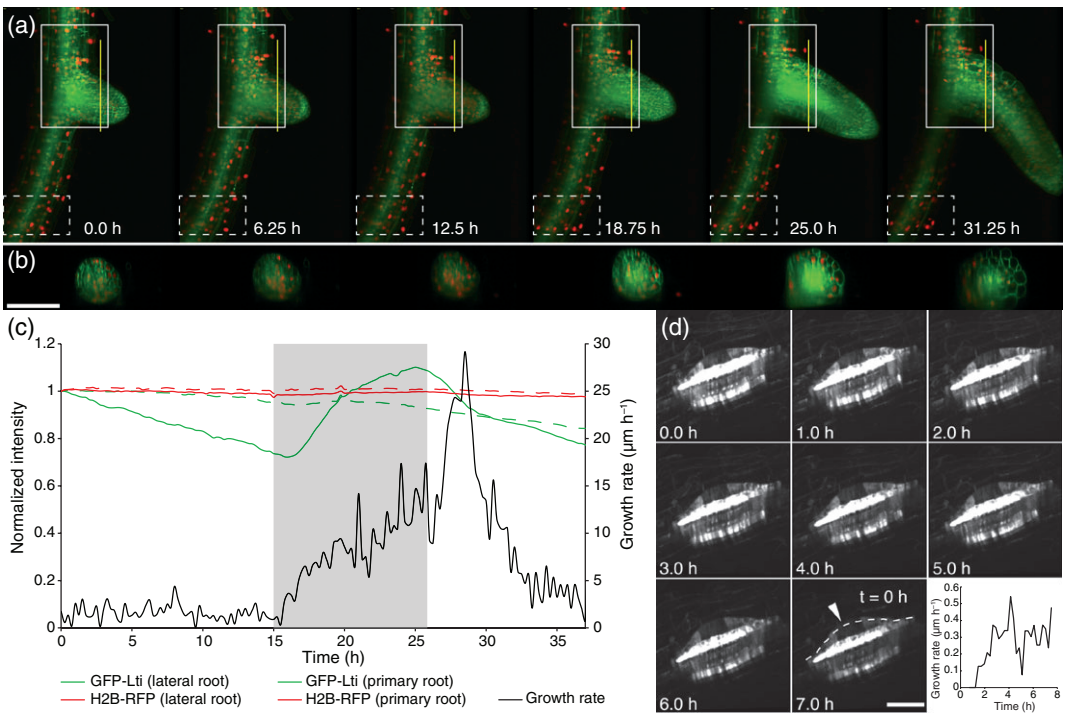

Figure 2. Light-sheet-based 4D imaging of growing *Arabidopsis thaliana* root.
Time lapse imaging of an *A. thaliana* lateral root. The 7-day-old seedling stably expresses H2B–red fluorescent protein (RFP) (red, nucleus label) and LTi6–GFP (green, membrane label) both under control of the 35S promoter. A stack was recorded every 15 min over a period of 38 h. Each stack consists of 233 planes each at a 1.29 μm *z*-spacing and a total volume of 335 μm × 449 μm × 300 μm (*x*/*y*/*z*). Images were taken with a Carl Zeiss C-Apochromat 20×/0.5 W objective lens for the detection and a Carl Zeiss EC Plan-Neofluar 5×/0.16 for illumination.
(A) Maximum-intensity projections of six indicated time points out of 151 are shown in the upper panel. The yellow line indicates the position of the optical transversal sections presented in (B). For each channel, the mean intensity in the white boxed areas (solid line and dashed line box) was measured in the average intensity projections, normalized to its initial intensity and plotted against time (C). The grey bar indicates the period during which the plant was illuminated. Scale bar: 100 μm. (D) Time-lapse imaging of a growing *A. thaliana* lateral root primordium. The primordium is labeled by an endoplasmic reticulum (ER)-localized GFP driven by the MIR390a promoter which is expressed specifically at the base and flanks of the developing primordium (Marin *et al.*, 2010). Stacks were recorded every 15 min for 7 h. Single planes of eight time points are shown. The dashed line in the 7 h panel points at the primordium at the onset of the recording. The increase in size is visualized by the arrowhead. The graph represents the average growth rate of the primordium over time. Scale bar: 25 μm. For both (A) and (B) the objective lenses were a Carl Zeiss N-Achroplan 20×/0.5 W for the detection and a Carl Zeiss EC Epiplan-Neofluar 2.5×/0.06 for illumination.

surge in growth rate (Figure 2C). By contrast the intensity of the H2B–RFP signal in the lateral root as well as the intensity of both fluorophores in the primary root stayed relatively constant over the observation period. This indicates that the change in fluorescence intensity observed for the plasma membrane marker reflects a lateral-root-specific event.

Even though more than 70 000 images were acquired, only moderate photobleaching could be observed (Figure 2C). Two observations indicate that the plant is behaving as expected in near physiological conditions. First, the wiggling movement of nuclei, traditionally seen in healthy plant cells (Van Bruaene *et al.*, 2003), was observed during the entire recording period (Movie S1). Second, we also recorded the growth of the primary root tip of a 7-day-old plant (Movie S2) over a period of 15 h measured at an average growth rate of 150 μm h^{-1}, which is similar to that reported in several studies (Beemster and Baskin, 1998; De Smet *et al.*, 2007). Taken together, this suggests that in our conditions the damage to the plant induced by handling and maintaining the plant in the chamber and during the entire imaging process can be kept to a minimum.

To further characterize lateral root development, we recorded the growth of a young lateral root primordium, which also illustrates the capability of light sheet microscopy to image structures located deeper inside the plant. In Arabidopsis, lateral roots form by the division of founder cells located in the pericycle, a cell layer that delineates the central vascular bundle of xylem and phloem and is located 40–50 μm from the plant root epidermis. The founder cells undergo several rounds of cell division to form a lateral root primordium, which will then grow out of the main root in a process called emergence. To identify young lateral root primordia, we took advantage of transgenic Arabidopsis plants expressing GFP under the control of the *MIR390a* promoter, a micro-RNA specifically expressed in the lateral root primordia (Marin *et al.*, 2010). We recorded a stage 4 (staging according to Malamy and Benfey, 1997) primordium for 7 h, taking pictures every 15 min (Figure 2D and

Movie S3). During that period, no cell divisions were observed, but the primordium continued to grow at an average rate of 0.3 μm h^{-1}. This indicates that cell division is not the sole driving force of lateral root growth and that cell expansion contributes too. Using the same reporter, we recorded the growth and emergence of a mature lateral root out of the primary root (Movie S4) for 30 h. There several cell divisions could be observed.

In summary, these results indicate that our DSLM setup allows the long-term imaging of plant growth and combines minimal invasiveness and a high signal-to-noise ratio with high planar and axial resolution.

Imaging at cellular and subcellular scales

The initiation and growth of whole organs are processes that span several hours and occur at scales of tens to hundreds of micrometers. Cell division in Arabidopsis occurs within <30 min and is characterized by the early selection of a division plane, which is marked by the appearance of the pre-prophase band prior to the division of the nucleus (Van Damme, 2009). We recorded the root tip of a transgenic Arabidopsis expressing constitutively a fusion between the microtubule-associated protein MAP4 and GFP for 1 h, acquiring a stack of 194 images every 2.5 min. During this period, at least six cell divisions occurred (Figure 3A, arrowheads and Movie S5) and could be resolved with excellent spatial and temporal resolution. The passage of the pre-prophase band and spindle formation (Figure 3B, 25–30 min) were clearly discernible.

Dynamics of the movement of subcellular organelles is a typically fast event. We recorded the movements of endosomal compartments labeled by a YFP-RabF2a reporter (Geldner *et al.*, 2009) (Figure 3C and Movie S6). Using a recording speed of 4 frames per second (fps) we successfully tracked a single endosome over 40 sec in a root hair cell. This endosome moved with an average speed of 1.7 μm sec^{-1} and showed maximum speed of up to 5.8 μm sec^{-1} (Figure 3D).

Using DSLM, cellular and subcellular biological processes, as they occur in the context of a developing organism, can be captured at high spatial resolution and various temporal scales.

Improved image quality by the use of structured illumination and multi-angle acquisition

The imaging of large, non-transparent specimens, such as developing multicellular organisms, is complicated by the decreased contrast due to light scattering. To improve the image quality, we took advantage of incoherent structured illumination (Keller *et al.*, 2010). Rather than illuminating the sample with a homogeneous light sheet, the intensity of the illuminating laser beam is modulated in synchrony with the scanning process. The sample is illuminated by stripes of light and an acquisition of a shift series of images at three spatial phases of this pattern allowed us to discriminate the scattered background light against signal fluorescence using a simple processing algorithm (Neil *et al.*, 1997). The gain in image quality was assayed by comparing the normalized intensities of images acquired with a continuous light sheet (LS) or a different pattern of structured illumination (SI) against the same region in the same sample. The application of SI improved the imaged quality significantly, providing a higher contrast with more visual features (Figure 4A–C). The type of SI pattern had an influence on the gain in image. A low number of modulations (<SI20) removes blurry parts at higher penetration depths (>50 μm) and increases the signal to background ratio. The contrast of surface structures is improved with a high number of modulations (>SI40) but can lead to a loss of signal. For our application, a good compromise between an optimum in contrast gain and an overall decrease in intensity is achieved with 40 modulations (SI40; Figure S3).

An intrinsic limitation of using the illumination from the side is the formation of stripes caused by the absorption of the illuminating light sheet and the consequent casting of shadow behind large fluorescent objects (e.g. Figure 2B). In our setup, the sample is mounted on a rotary stage. This allows us to acquire image stacks of the same specimen along multiple directions (multi-angle views). The two to six views are computationally registered and fused generating a single final image stack. This method increases the overall information obtained from a single view and reduces the optical artifacts caused by the shadows (Verveer *et al.*, 2007). To illustrate this effect, we recorded stacks of images of a single root tip along five different directions (30° apart) and combined the five views (Figure 4D). Compared with a single view acquisition, in which the cell contours located further away from the light sheet were poorly resolved, the multi-view image properly reconstructed and resolved all cells in the sample (Figure 4D).

DISCUSSION

We used light-sheet-based fluorescence microscopy to image the development of living transgenic Arabidopsis plants expressing fluorescent markers. The plants were oriented vertically in a specially designed chamber, which provides close-to-standard laboratory growth conditions. The growth of the root meristem and of lateral organs was recorded for up to 38 h without any obvious signs of damage. We consistently achieved very good planar and axial resolution. We also recorded cellular and subcellular events in the whole organism on time scales from seconds to minutes. The application of structured illumination and multi-angle acquisition further improved the image quality.

By following the growth of a lateral root, we observed that its growth rate was variable (Figure 2C) and coincided with the periods during which the plant was illuminated. The growth rate peaked at dusk, reminiscent of the diurnal

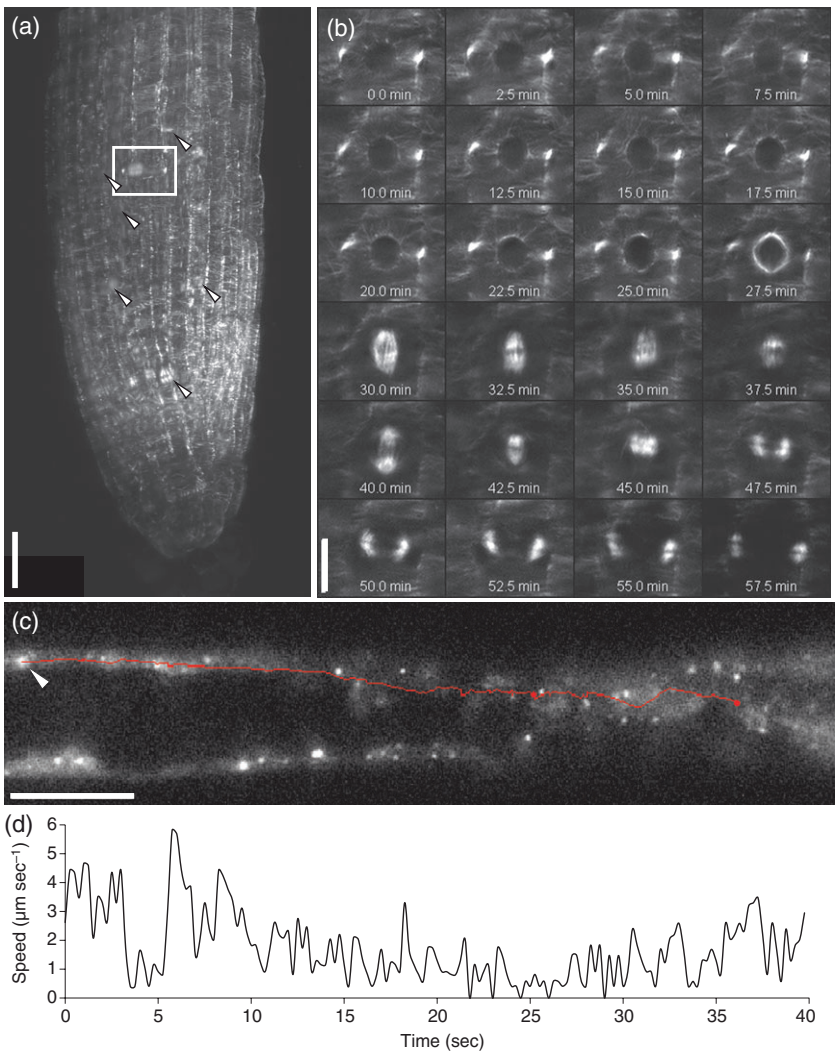

Figure 3. Four-dimensional imaging of cellular and subcellular features using digital scanned laser light sheet fluorescence microscopy (DSLM) imaging.
(A) Maximum-intensity projection of a DSLM time-lapse recording of a microtubule labeled 4-day-old Arabidopsis root expressing GFP–MAP4. Cell divisions are indicated by arrowheads.
(B) A DSLM time-lapse recording of the division of a single root cortex cell. Each picture corresponds to the boxed area in (A) and represents a single plane located 19.5 μm deep into the root (cortical layer). Images were taken every 2.5 min for 1 h with a Carl Zeiss N-Achroplan 40×/0.75 W objective lens for the detection and a Carl Zeiss EC Plan-Neofluar 5×/0.16 for illumination with structured illumination (SI10). The images were then deconvoluted. Each stack contains 194 planes recorded at a 0.645 μm *z*-spacing and a total volume of 168 μm × 224 μm × 125 μm (*x*/*y*/*z*).
(C) The first time point of a single plane time-lapse recording of an Arabidopsis root hair. The 6-day-old plant expresses the late endosome marker YFP–RabF2a (Geldner *et al.*, 2009). The colored line indicates the track of one endosome in a time frame 40 sec. Its speed over the time is shown in (D). Images were recorded at a rate of 4 frames per second for a 40 sec stretch with a Carl Zeiss N-Apochromat 63×/1.0 W objective lens for the detection and a Carl Zeiss EC Plan-Neofluar 5×/0.16 for illumination. The tracking was performed with ImageJ using the Manual Tracking plugin.
Scale bar: (A) 20 μm; (B, C) 10 μm.

growth rhythm displayed by the shoot (Nozue *et al.*, 2007) but opposite to the pattern displayed by the primary root, peaking at dawn (Yazdanbakhsh and Fisahn, 2010). We observe that during early development of lateral root primordia, cell proliferation was not the sole driving force of growth but that cell expansion contributed too (Figure 2D). It was never reported that, in between cell divisions, young primordia were elongating, a process thought to occur only in more mature primordia upon emergence (Malamy and Benfey, 1997).

A prominent feature of light-sheet-based fluorescence microscopy for imaging of plant growth is its versatility. Aerial and root tissues can be imaged with comparable quality over time periods ranging from seconds to several days. The scale of the structures that can be imaged ranges from whole organs (several hundreds of micrometers) to organelles (sub-micrometer). Image quality was consistently very good at all scales.

The correct quality and type of lenses used for illumination and detection is vital to achieve good spatial resolution.

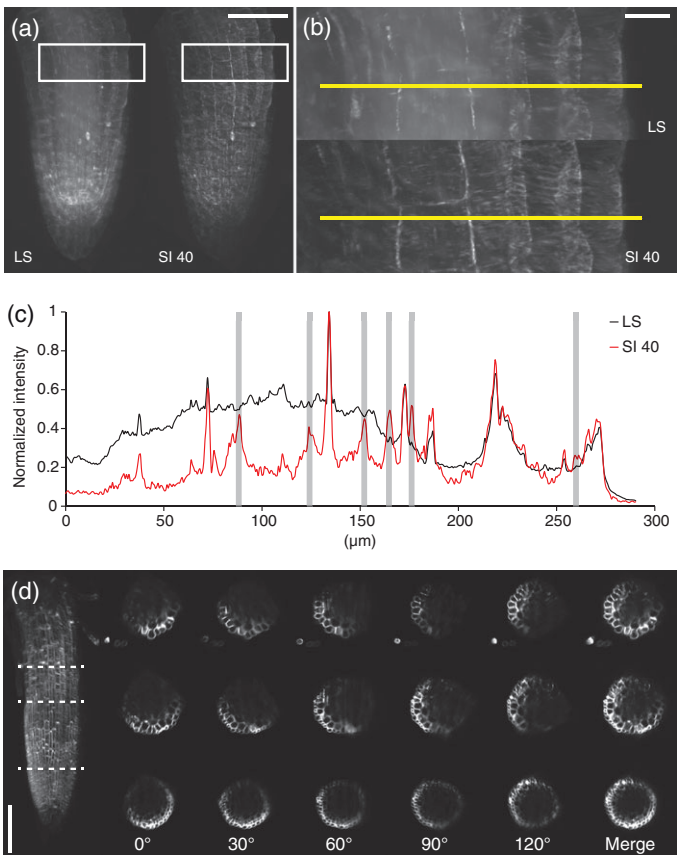

Figure 4. Enhancing image contrast with structured illumination and multi-view imaging.
(A) Maximum-intensity projections of a 4-day-old Arabidopsis root expressing the microtubule marker MAP4–GFP (Marc *et al.*, 1998) recorded with standard light sheet illumination (LS) and structured illumination (SI40). The boxed area indicates the magnified region in (B).
(B) Maximum-intensity projections at standard light sheet illumination (LS) and structured illumination (SI 40). The line indicates the position of the intensity profile depicted in (C).
(C) Intensity plot along the lines indicated in (B). In both plots, the raw intensity values were normalized by the maximum intensity in each image. Shading highlights features in the structured illumination image that are not visible in the light sheet mode image. Images show a maximum projection of 187 planes with a 0.645 μm *z*-spacing and a total volume of 168 μm × 224 μm × 120 μm (*x*/*y*/*z*). They were taken with a Carl Zeiss N-Achroplan 40×/0.75 W objective lens for detection and a Carl Zeiss EC Plan-Neofluar 5×/0.16 for illumination. Images were deconvoluted. The light sheet enters the specimens from the right of the picture.
(D) The digital scanned laser light sheet fluorescence microscopy (DSLM)-SI multiple-view recording of a membrane-labeled 4-day-old root expressing LTi–GFP. The five angles of acquisition were aligned using Amira and are shown as maximum intensity projection on the right. The dashed lines indicate the position of the optical transverse section presented in the panel showing each angle of acquisition and the maximum projection merge. Images were taken with a Carl Zeiss C-Apochromat 20×/0.5 W objective lens for detection and a Carl Zeiss EC Epiplan-Neofluar 2.5×/0.06 for illumination; each stack contains 311 planes with 1.29 μm *z*-spacing and a total volume of 335 μm × 449 μm × 401 μm (*x*/*y*/*z*).
Scale bars: (A) 50 μm; (B) 10 μm; (D) 100 μm.

The use of high-quality (high-numerical aperture) lenses is essential. Depending on the size of the object, we used different combinations of lenses for detection and illumination. The properties of the detection system determine the lateral (*x*/*y*-axes) resolution while the properties of the illumination system determine the thickness of the light sheet, and therefore the axial resolution (*z*-axis). For imaging whole organs such as root or shoot tips, a 2.5×/0.06 lens for illumination (approximate thickness of light sheet 5 μm) and a 20×/0.5 for detection were optimal, while a 5×/0.16 for illumination (approximate thickness of light sheet 2 μm) was better suited for the smaller lateral root primordia. To capture events at the cellular scale, we chose a combination of 5×/0.16 (illumination) and 40×/0.75 (detection) and a combination of 5×/0.16 (illumination) and 63×/1.0 (detection) for subcellular events. We used several methods to further improve image quality. The gain achieved by deconvolution was significant at most scales but relies on the correct acquisition of *z*-stacks. Most stacks of images were recorded at a rate of 4–5 fps, which is only sufficient if a temporal resolution in the minute range is acceptable. Structured illumination removes the blurriness caused by the scattered background light in thick samples and yields better-resolved images at the expense of a general drop in signal intensity and illumination of the sample by more light for each image (for SI, three images at different phases are combined to provide the final image). Finally, shadowing caused by the absorption of the illuminating light sheet in a thick sample

can be reduced by multi-angle acquisition and provides a more homogeneous resolution around the sample. This method results in a slower acquisition frequency due to the rotation of the stage between each view and entails the post-processing of the data to register each view and combine them. In our system, the fastest acquisition rate was of 4 fps, which did not take full advantage of the CCD camera. Applying appropriate settings for binning increases the frequency of image acquisition to well above 20 fps.

Compared with confocal microscopy, our approach presents several advantages for studying plant growth. The main benefit resides in the near physiological imaging conditions and the significantly reduced invasiveness of the image acquisition process over state-of-the-commercial-art technologies such as confocal fluorescence microscopy. In our design, plants are placed vertically in the microscope chamber, their roots grow in or on the surface of a gel while the aerial part is in the air. We have paid particular attention to the design of the sample holders, which ensure good stability over time and reduce the stress on the plant quite dramatically. The use of a perfusion system and of a sun-like light source illuminating the leaves renders the imaging conditions close to the standard growth conditions used in a plant laboratory. Most instances of recording plant growth using confocal microscopy rely either on putting the sample back into the growth chamber in between successive image acquisitions (Reddy *et al.*, 2004; Heisler *et al.*, 2005; Hamant *et al.*, 2008) or maintaining the plants between a cover-slip and a slide or agar-block (Laskowski *et al.*, 2008; Rybel *et al.*, 2010). In these cases, no compromise between not stressing the plant and being able to image at short interval can be found. In addition, confocal imaging is, in most cases (for an exception see Kleine-Vehn *et al.*, 2010), performed with the sample placed horizontally, which, as plant growth is highly influenced by gravity, can be problematic for long-term imaging.

Light sheet fluorescence microscopy opens several new avenues for the study of plant development. First, it allows for very low-invasive, high-resolution, time-resolved imaging of plant growth as well as studies of protein or gene expression dynamics at various long to short time scales. Second, combined with segmentation and tracking methodology, it allows the extraction of quantitative information on growing organs, which is essential for our understanding of morphogenesis and growth patterns at cellular resolution. Finally, in connection with nanosurgical procedures (Colombelli *et al.*, 2009), the effects of local perturbation in cell properties on morphogenesis will become accessible.

EXPERIMENTAL PROCEDURES

Plant growth conditions

Seeds were sterilized using 10% Natriumhypochlorid with 0.1% TritonX-100 in *aqua destilata* and rinsed with sterile distilled water. The seeds were germinated on 0.7% Phytagel plates supplemented with half-strength MS medium at pH 5.8 and transferred to the sample holder after 2 days. Plants were grown in a growth chamber (Percival Scientific, http://www.percival-scientific.com/) with 16 h light per 24 h day at 21°C.

Plant material

The following transgenic plants were used *p35S:GFP-MAP4* (Marc *et al.*, 1998), *pUBQ10:YFP-RabF2a* (Geldner *et al.*, 2009), pMIR390a:GUS-GFP (Marin *et al.*, 2010). The p35S:H2B-RFP/p35S:GFP-LTi6 was created by crossing plants bearing *p35S:H2B-RFP1* (Boisnard-Lorig *et al.*, 2001) (FF, L. Dupuy, Scottish Crops Research Institute, Dundee, Scotland, L. Laplaze, Institut de Recherche pour le Développement, Montpellier, France, M. Heisler, EMBL, Heidleberg, Germany and JH, unpublished data), with *p35S:GFP-LTI6b* (Kurup *et al.*, 2005). Homozygous lines that showed no evidence of silencing were screened using a Leica MZFLIII epifluorescence stereomicroscope (http://www.leica.com/).

Imaging conditions

All microscope image acquisitions were performed on the mDSLM, which is a heavily improved version of the DSLM described in Keller *et al.* (2010). The following laser lines and filter sets were used. The GFP and yellow fluorescent protein (YFP) were excited at 488 nm by a diode laser and detected between 500 and 550 nm. Red fluorescent protein was excited at 561 nm by a diode-pumped solid state (DPSS) laser and detected between 572 and 642 nm. The detection lenses that were used are described in each figure legend. Images were acquired by a high-resolution interline CCD camera (Andor Clara, http://www.andor.com/; pixel size 6.45 μm). The chamber is equipped with a perfusion system (ISMATEC, http://www.ismatec.com/; model ISM 832c), which was used only for long-term (>2 h) observations. It exchanges the chamber volume of 13 ml within 15 min. The inflow is placed at the bottom and the outflow at the top of the microscope chamber. Before each session, the performance of the microscope was checked with standardized multi-fluorescent microspheres (0.2 μm diameter, Invitrogen T7280, http://www.invitrogen.com/) embedded in a 1.0% agarose cylinder and with the biological specimen.

Post-processing and image analysis

Image analysis and post-processing were carried out with ImageJ (http://rsbweb.nih.gov/ij/). The deconvolution was performed using the parallel iterative deconvolution 3D plugin in ImageJ using a PSF created with the ImageJ plugin Diffraction PSF 3D. Endosome tracking was performed using the ManualTracking plugin in ImageJ. The registration of the multi-angle acquisition was carried out with Amira (Visage Imaging Inc., http://www.visageimaging.com/). The root growth rate was measured using Adobe After Effects. First a drift correction was performed by tracking the matured primary root. Then the growing root tip was tracked. Its position over time was calculated as the growth rate for every given time point.

ACKNOWLEDGEMENTS

We thank B. Höckendorf and A. Leibfried for their critical reading. We thank M. Heisler for the MAP4-GFP line. We are grateful to P. Theer, A. Atzberger, F. Härle and A. Riedinger for their contributions to the mDSLM. This work was supported by the Land Baden-Württemberg, the Chica und Heinz Schaller Stiftung and the CellNetworks cluster of excellence (AM). DvW and ESt are funded by the Center of Excellence at Frankfurt for Macromolecular Complexes (CEF-MC) and the Deutsche Forschungsgemeinschaft (DFG). FF and

JH are funded by the Gates Foundation and Engineering and Physical Sciences Research Council (EPSRC).

SUPPORTING INFORMATION

Additional Supporting Information may be found in the online version of this article:

Figure S1. Growth chambers used for plant growth.

Figure S2. Optical properties of Phytagel.

Figure S3. Gain in image quality for different SI pattern.

Movie S1. Time-lapse recording of a growing Arabidopsis lateral root.

Movie S2. Time-lapse recording of an Arabidopsis primary root tip.

Movie S3. Time-lapse recording of elongating lateral root primordium.

Movie S4. Time-lapse recording of a lateral root emerging from the main root.

Movie S5. Time-lapse recording of root epidermal cell division.

Movie S6. Single plane time-lapse recording of endosomes in Arabidopsis root hair.

Please note: As a service to our authors and readers, this journal provides supporting information supplied by the authors. Such materials are peer-reviewed and may be re-organized for online delivery, but are not copy-edited or typeset. Technical support issues arising from supporting information (other than missing files) should be addressed to the authors.

REFERENCES

Beemster, G. T. and Baskin, T. I. (1998) Analysis of cell division and elongation underlying the developmental acceleration of root growth in *Arabidopsis thaliana*. *Plant Physiol.* **116**, 1515–1526.

Boisnard-Lorig, C., Colon-Carmona, A., Bauch, M., Hodge, S., Doerner, P., Bancharel, E., Dumas, C., Haseloff, J. and Berger, F. (2001) Dynamic analyses of the expression of the HISTONE::YFP fusion protein in arabidopsis show that syncytial endosperm is divided in mitotic domains. *Plant Cell*, **13**, 495–509.

Colombelli, J., Besser, A., Kress, H., Reynaud, E. G., Girard, P., Caussinus, E., Haselmann, U., Small, J. V., Schwarz, U. S. and Stelzer, E. H. (2009) Mechanosensing in actin stress fibers revealed by a close correlation between force and protein localization. *J. Cell Sci.* **122**, 1665–1679.

De Smet, I., Tetsumura, T., De Rybel, B. *et al.* (2007) Auxin-dependent regulation of lateral root positioning in the basal meristem of Arabidopsis. *Development*, **134**, 681–690.

Engelbrecht, C. J., Greger, K., Reynaud, E. G., Krzic, U., Colombelli, J. and Stelzer, E. H. (2007) Three-dimensional laser microsurgery in light sheet based microscopy (SPIM). *Opt. Express*, **15**, 6420–6430.

Fang, Y. and Spector, D. L. (2005) Centromere positioning and dynamics in living Arabidopsis plants. *Mol. Biol. Cell*, **16**, 5710–5718.

Geldner, N., Dénervaud-Tendon, V., Hyman, D. L., Mayer, U., Stierhof, Y. D. and Chory, J. (2009) Rapid, combinatorial analysis of membrane compartments in intact plants with a multicolor marker set. *Plant J.* **59**, 169–178.

Hamant, O., Heisler, M. G., Jönsson, H. *et al.* (2008) Developmental patterning by mechanical signals in Arabidopsis. *Science*, **322**, 1650–1655.

Heisler, M. G., Ohno, C., Das, P., Sieber, P., Reddy, G. V., Long, J. A. and Meyerowitz, E. M. (2005) Patterns of auxin transport and gene expression during primordium development revealed by live imaging of the Arabidopsis inflorescence meristem. *Curr. Biol.* **15**, 1899–1911.

Heisler, M. G., Hamant, O., Krupinski, P., Uyttewaal, M., Ohno, C., Jönsson, H., Traas, J. and Meyerowitz, E. M. (2010) Alignment between PIN1 polarity and microtubule orientation in the shoot apical meristem reveals a tight coupling between morphogenesis and auxin transport. *PLoS Biol.* **8**, e1000516.

Keller, P. J., Schmidt, A. D., Wittbrodt, J. and Stelzer, E. H. (2008) Reconstruction of zebrafish early embryonic development by scanned light sheet microscopy. *Science*, **322**, 1065–1069.

Keller, P. J., Schmidt, A. D., Santella, A., Khairy, K., Bao, Z., Wittbrodt, J. and Stelzer, E. H. (2010) Fast, high-contrast imaging of animal development with scanned light sheet-based structured-illumination microscopy. *Nat. Methods*, **7**, 637–642.

Kleine-Vehn, J., Ding, Z., Jones, A. R., Tasaka, M., Morita, M. T. and Friml, J. (2010) Gravity-induced PIN transcytosis for polarization of auxin fluxes in gravity-sensing root cells. *Proc. Natl Acad. Sci. USA*, **107**, 22344–22349.

Kurup, S., Runions, J., Köhler, U., Laplaze, L., Hodge, S. and Haseloff, J. (2005) Marking cell lineages in living tissues. *Plant J.* **42**, 444–453.

Laskowski, M., Grieneisen, V. A., Hofhuis, H., Hove, C. A., Hogeweg, P., Marée, A. F. and Scheres, B. (2008) Root system architecture from coupling cell shape to auxin transport. *PLoS Biol.* **6**, e307.

Malamy, J. E. and Benfey, P. N. (1997) Organization and cell differentiation in lateral roots of *Arabidopsis thaliana*. *Development*, **124**, 33–44.

Marc, J., Granger, C. L., Brincat, J., Fisher, D. D., Kao, T. h., McCubbin, A. G. and Cyr, R. J. (1998) A GFP-MAP4 reporter gene for visualizing cortical microtubule rearrangements in living epidermal cells. *Plant Cell*, **10**, 1927–1940.

Marin, E., Jouannet, V., Herz, A., Lokerse, A. S., Weijers, D., Vaucheret, H., Nussaume, L., Crespi, M. D. and Maizel, A. (2010) miR390, Arabidopsis TAS3 tasiRNAs, and their AUXIN RESPONSE FACTOR targets define an autoregulatory network quantitatively regulating lateral root growth. *Plant Cell*, **22**, 1104–1117.

McNally, J. G., Karpova, T., Cooper, J. and Conchello, J. A. (1999) Three-dimensional imaging by deconvolution microscopy. *Methods*, **19**, 373–385.

Neil, M. A., Juskaitis, R. and Wilson, T. (1997) Method of obtaining optical sectioning by using structured light in a conventional microscope. *Opt. Lett.* **22**, 1905–1907.

Nozue, K., Covington, M. F., Duek, P. D., Lorrain, S., Fankhauser, C., Harmer, S. L. and Maloof, J. N. (2007) Rhythmic growth explained by coincidence between internal and external cues. *Nature*, **448**, 358–361.

Paredez, A. R., Somerville, C. R. and Ehrhardt, D. W. (2006) Visualization of cellulose synthase demonstrates functional association with microtubules. *Science*, **312**, 1491–1495.

Reddy, G. V., Heisler, M. G., Ehrhardt, D. W. and Meyerowitz, E. M. (2004) Real-time lineage analysis reveals oriented cell divisions associated with morphogenesis at the shoot apex of *Arabidopsis thaliana*. *Development*, **131**, 4225–4237.

Rybel, B. D., Vassileva, V., Parizot, B. *et al.* (2010) A novel Aux/IAA28 signaling cascade activates GATA23-dependent specification of lateral root founder cell identity. *Curr. Biol.* **20**, 1697–1706.

Swarup, R., Kramer, E. M., Perry, P., Knox, K., Leyser, H. M., Haseloff, J., Beemster, G. T., Bhalerao, R. and Bennett, M. J. (2005) Root gravitropism requires lateral root cap and epidermal cells for transport and response to a mobile auxin signal. *Nat. Cell Biol.* **7**, 1057–1065.

Van Bruaene, N., Joss, G., Thas, O. and Van Oostveldt, P. (2003) Four-dimensional imaging and computer-assisted track analysis of nuclear migration in root hairs of *Arabidopsis thaliana*. *J. Microsc.* **211**, 167–178.

Van Damme, D. (2009) Division plane determination during plant somatic cytokinesis. *Curr. Opin. Plant Biol.* **12**, 745–751.

Verveer, P. J., Swoger, J., Pampaloni, F., Greger, K., Marcello, M. and Stelzer, E. H. (2007) High-resolution three-dimensional imaging of large specimens with light sheet-based microscopy. *Nat. Methods* **4**, 311–313.

Wohland, T., Shi, X., Sankaran, J. and Stelzer, E. H. (2010) Single plane illumination fluorescence correlation spectroscopy (SPIM-FCS) probes inhomogeneous three-dimensional environments. *Opt. Express* **18**, 10627–10641.

Yazdanbakhsh, N. and Fisahn, J. (2010) Analysis of *Arabidopsis thaliana* root growth kinetics with high temporal and spatial resolution. *Ann. Bot.* **105**, 783–791.